

## A Study of the mechanical properties of aluminum composite materials prepared by atomization process

Harith Ibrahim Jaffer <sup>a</sup> Ekram Atta Al-Ajaj <sup>a</sup>  
Sadeem Abbas Fadhil <sup>a,\*</sup>

<sup>a</sup> University of Baghdad/ College of Science/ Department of Physics  
Email: [physifriend@yahoo.com](mailto:physifriend@yahoo.com)

### Abstract

Steel fiber aluminum matrix composites were prepared by atomization technique. Different air atomization conditions were considered; which were atomization pressure and distance between sample and nozzle. Tensile stress properties were studied. XRF and XRD techniques were used to study the primary compositions and the structure of the raw materials and the atomized products. The tensile results showed that the best reported tensile strength observed for an atomization pressure equal to 4 mbar and sample to nozzle distance equal to 12 cm. Young modulus results showed that the best result occurred with an air atomization pressure equal to 8 mbar and sample to nozzle distance equal to 16cm.

### Key words

MMCs, Atomization, Tensile.

### Article info

Received: Oct. 2010

Accepted: Apr. 2011

Published: Oct. 2011

### دراسة الخواص الميكانيكية لمتراكبات الألمنيوم المحضرة بطريقة التذرية

حارث ابراهيم جعفر\*      اكرام عطا العجاج\*  
سديم عباس فاضل\*

\*جامعة بغداد/ كلية العلوم/ قسم الفيزياء

### الخلاصة:

تم تحضير متراكبات أساس الألمنيوم المدعمة بألياف الفولاذ بطريقة التذرية. تم أخذ ظروف مختلفة لعملية التذرية بنظر الاعتبار وهي ضغط التذرية و المسافة بين العينة والمرذاذ. درس التأثير على خواص اجهاد الشد. تقنيات فلورة الأشعة السينية و حيود الأشعة السينية استخدمت لدراسة التركيب الأولي و الخواص التركيبية للمواد الأولية والمواد الناتجة من التريذ. أظهرت نتائج الشد ان أفضل نتيجة موثقة لحد المرونة لوحظت عند ضغط تذرية يساوي 4 mbar و عند بعد للعينة من المرذاذ يساوي 12 cm . أما لمعامل يونك فكانت عند ضغط تذرية باستخدام الهواء يساوي 8 mbar و عند بعد للعينة من المرذاذ يساوي 16 cm .

### Introduction

Metal–matrix composites (MMCs) of the key research subjects in materials science during the past two decades. Most of the work has been dealing with aluminum and other light metal matrixes for application requiring lightweight in combination with high strength and/or stiffness [1, 2]. Spray processes aim at taking advantage of the increased surface area at the interface that

results from breaking up a bulk material, either liquid (during processing) or solid (prior to processing), into a large number of smaller pieces (particles/droplets). As heat and mass transfer (including chemical reactions) between two different physical phases (e.g., liquid/gas, solid/gas) occur at the interface between the two phases, increasing the surface area of that interface enhances the rate at which these exchanges can occur.

Atomization spray is a molten processing technique that allows production of unusual structures and superior properties for alloys and composites [2]. In this process the material is melted and atomized into droplets before impinging onto a substrate. The droplet may be collected in a mould, on to a circulating disk, strip, or a rotating shaft, where solidification occurs. It is benefit to list some of the related work in this field like: Gupta *et al.* [3] in 2006 synthesized a novel aluminum-based hybrid composite containing titanium particulates (discontinuous/particulates reinforcement) and iron mesh (continuous /interconnected reinforcement) using a solidification processing route involving disintegrated melt deposition coupled with hot extrusion. Microstructural characterization studies revealed reduced grain size ( $\approx 44\%$ ) when compared to monolithic aluminum, uniform distribution of unreacted and reacted titanium in matrix, and absence of reaction products at the iron-wire/aluminum matrix interface. The mechanical showed that, elastic modulus increased by approximately 10%, 0.2% yield strength increasing by 20% and ultimate tensile strength increasing by approximately 27%. Zhang *et al.* in 2008 [4] fabricated fiber reinforced aluminum matrix composite, based on powder metallurgy (PM). The reinforced fiber was in situ synthesized during hot extrusion procedure of a mixed pure metal powders compact of Al–10 wt % Mg. The tensile stress–strain curve of in situ Al-MMCs involved a remarkable nonlinear deformation region and a long yield plateau region, and the reason was believed to result from deformation induced phase transition of  $\text{Al}_3\text{Mg}_2$ . The yield strength  $\sigma_{0.2}$ , tensile strength and elongation of in situ Al-MMCs was 137 MPa, 147 MPa and 7.0%, respectively. Mandal *et al.* [5] in 2008 prepared pure Al base short steel fiber reinforced composites by stir casting method. Steel

fibers were coated with copper and nickel by electroless deposition method. The density, hardness and strength of composites increased as compared to matrix alloy. The mechanical properties of these composites were measured and the results were correlated with the microstructure observation. It was found that copper-coated short steel fiber reinforced composites show considerable improvement in strength with good ductility because copper form a good interface between Al matrix and short steel fiber. Nickel-coated steel fiber reinforced composites showed improvement in strength to a lower extent possibly because of formation of intermetallic compound at the interface. The improvement in strength with uncoated fibers and nickel-coated fibers is on the lower side because of formation of brittle intermetallic compounds like  $\text{Fe}_2\text{Al}_5$  and  $\text{FeAl}_3$ . Fracture surface of tensile specimen was examined with SEM, which revealed a ductile fracture. Copper coating on steel fiber improved the strength properties while retaining a high level of ductility due to better interface bonding.

### System and Atomization process

The atomization apparatus is as shown in Fig. (1). Spray-deposition processes start from a solid bulk material that is heated (inductively or conductively) in a crucible Fig. (2). Aluminum and iron alloys make up the bulk of spray-deposited materials but copper and magnesium alloys as well as superalloys have also been successfully processed using this technique. The melt is disintegrated into a fine dispersion of droplets to form a spray (dispersed liquid phase) using high-energy gas jets (e.g., Ar, He,  $\text{N}_2$ ) with velocities ranging from subsonic (50 m/s) to supersonic (up to 500 m/s).



Fig. (1) The atomization apparatus used in preparation.

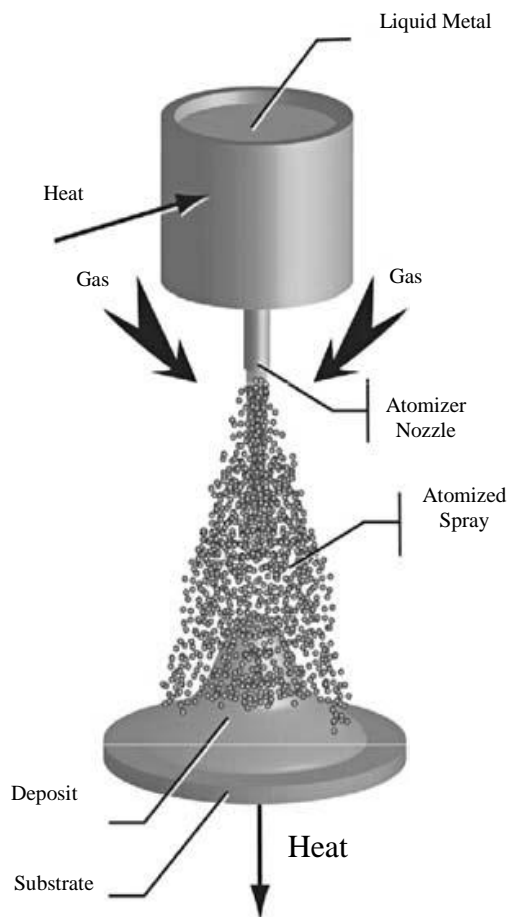


Fig. (2) Sketch of the spray atomization and deposition process [2].

During their trajectory toward the target (stationary or mobile), the droplets undergo convective cooling, partial rapid solidification, and possibly chemical

reaction with the surrounding atmosphere. They finally impinge on the target (ideally while still in a partially solidified state) where they consolidate into a deposit (or preform) [2]. In the present work the effect of two atomization parameters on the tensile properties are studied:

1. The atomization pressure.
2. The distance between nozzle and specimen. Nine samples were taken here.

### Raw materials and samples preparation

The Materials used here are basically aluminum 2024 as a raw material, which brought from local market as rods. XRF and XRD are taken for these rods in the ministry of Science and Technology; Shimadzu-labx X-ray diffraction unit model XRD-6000, kV = 40, Cu k $\alpha$ , and XRF (EDXRF) type, Twin-X, Oxford co. England. XRF results are shown in Table (1). XRD spectrum for these rods is shown in Fig. (3) and for the air atomized aluminum is shown in Fig. (4). XRF shows that the used fiber is steel carbon alloy fiber as in Table (1). The aluminum composite has been prepared using apparatus that shown in Fig. (1).

Table (1) Raw materials elementary composition.

Sample type	Elementary composition	Percentage %
Al-2024	Mn	0.24
	Fe	0.40
	Ni	0.11
	Cu	4.21
	Zn	0.15
	Al	The rest
Steel Carbon	V	0.01
	Cr	0.1
	Mn	0.44
	Fe	97.72
	Ni	0
	Cu	0
	Mo	0.05

The furnace temperature is subsequently increased up to the preset temperature, 750°C, by means of the temperature controller brought from local market.

After being weighted the alloy pieces were placed inside the crucible via upper orifice of the furnace. Before atomization, fiber mesh is put and fixed on a perforated 30 cm square iron plate by means of wires from the same fiber mesh material which is steel carbon alloy. These wires give benefits in tighten the fiber mesh with the plate by making the wires pass through the orifices then tighten to the fiber. This process helps in minimizing the pores inside the sample after atomization process. After that the iron sheet with fiber are put on a controlled rotating end. The atomization process is done by making air flow to the nozzle at certain atomization pressure. Subsequently, the crucible orifice is opened in order to flow and accumulate the atomized molten metal on a rotating iron sheet that contains the fiber mesh. The atomized molten metal impinges on the sheet and trapped by the fiber. The quantity of the atomized aluminum is adjusted so that the atomized aluminum completely filled the spaces in between the fiber mesh up to completely covering the fiber mesh. After finishing one face of the sample it's turned up down and the other face is put under atomization under the same atomizing conditions. After that the sample is prepared for testing and measurement. The samples are then cut and grinded and prepared to the tensile test according to the ASTM B 557M-06. the samples put under tensile test using H50KT, Tinius Olsen device. Different composites are prepared under different conditions as shown in Table (2).

Table (2) the names and preparation condition of samples.

Sample name	Sample distance (cm)	Atomization pressure (mbar)
AS110	12	8
AS29	12	8
AS32	12	5
AS43	12	4
AS58	14	8
AS64	16	3
AS76	16	8
AS85	18	6
AS97	18	8

The as atomized sample is shown in Fig. (3) and the grinded sample prepared for tensile test is shown in Fig. (4).

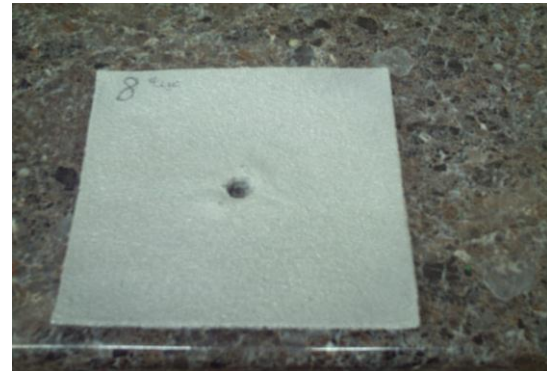


Fig. (3): the as atomized sample AS58 , with atomization pressure 8 mbar and distance between sample and nozzle is 14 cm.

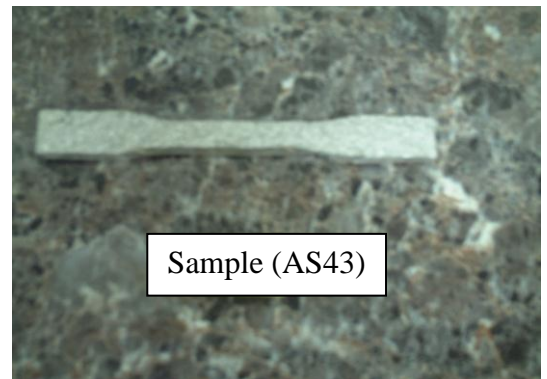


Fig. (4) Grinded sample prepared for tensile test.

## Results

XRD spectrum taken for the raw material and the sprayed sample are shown in Fig. (5) and (6) respectively. Different values of atomization pressures and different distances between nozzle and specimen were taken and the stress-strain curves were shown in Figs. (7-15) for different conditions.

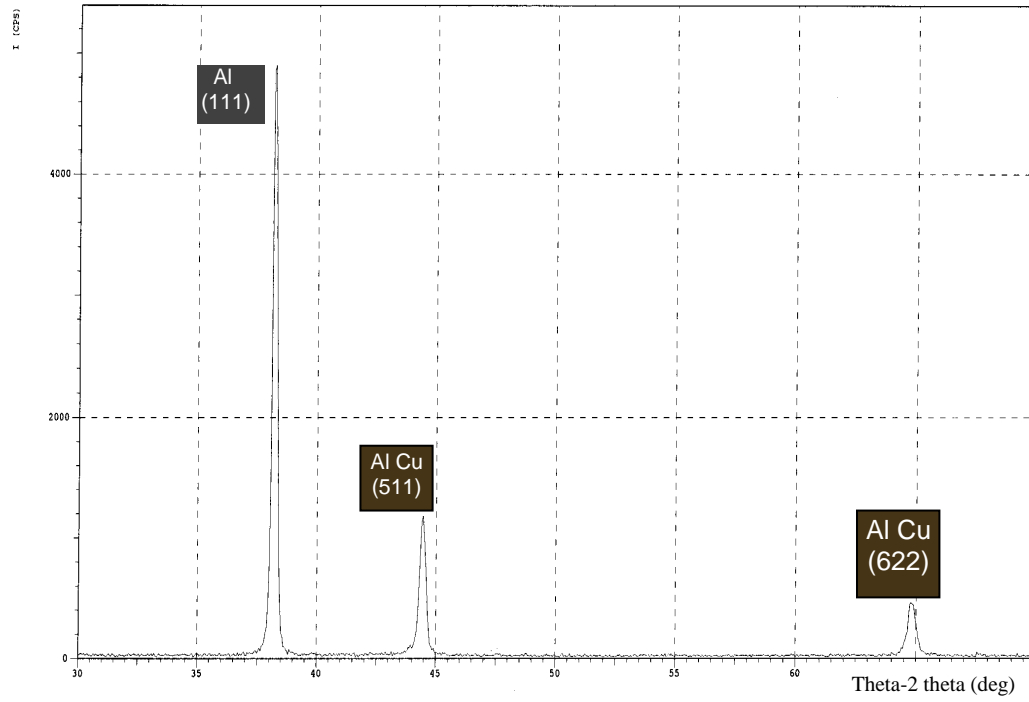


Fig. (5): XRD spectrum for the aluminum rods used as raw material.

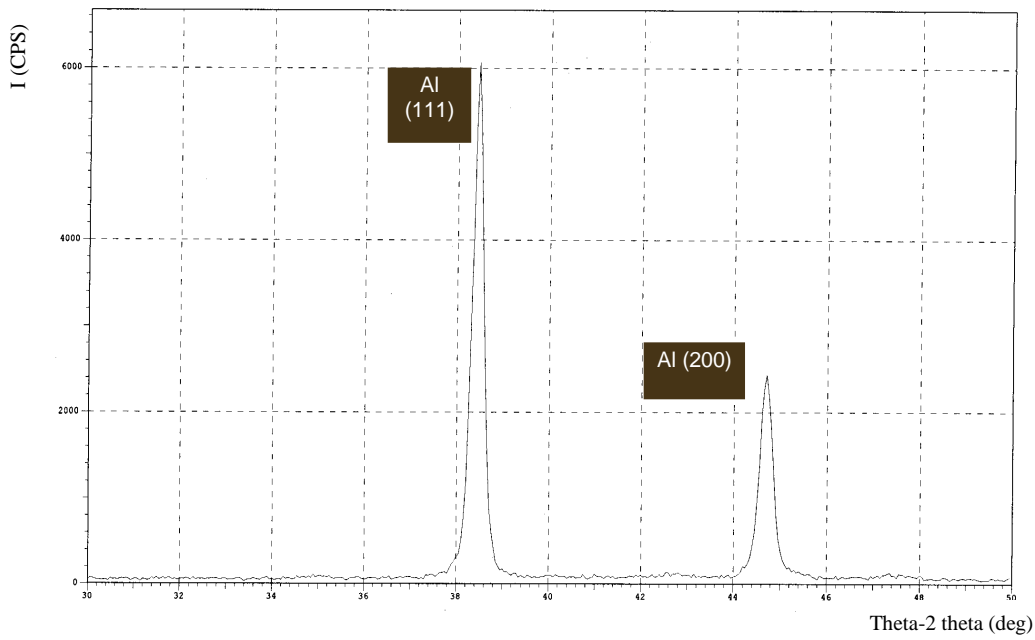


Fig. (6): XRD spectrum of the atomized aluminum.

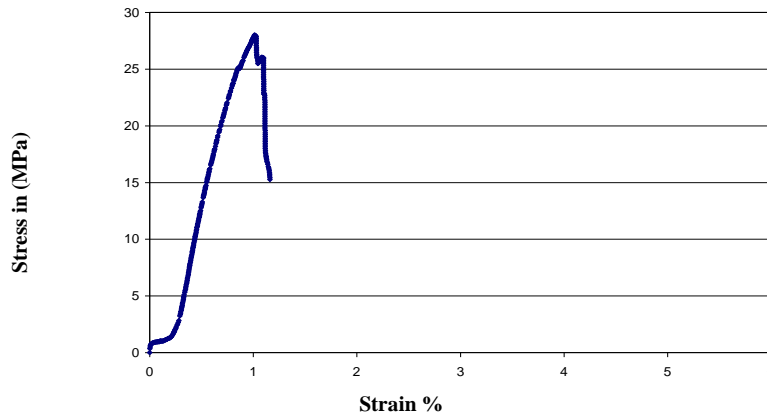


Fig. (7) Stress strain curve of Aluminum only Sample (AS110), Atomization pressure =8 mbar distance from nozzle =12 cm.



Fig. (8) Stress strain curve of Sample (AS29) Atomization pressure =8 mbar distance from nozzle =12 cm.

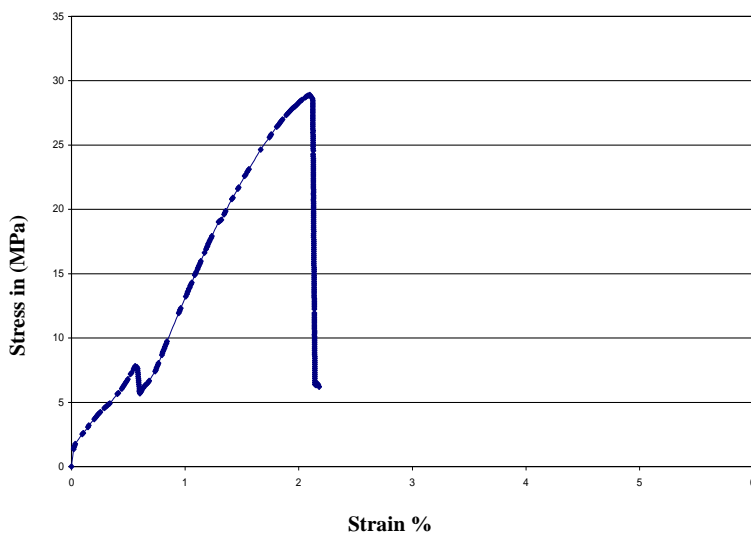


Fig. (9) Stress-strain curve of sample (AS32), atomization pressure =5 mbar distance from nozzle =12 cm.

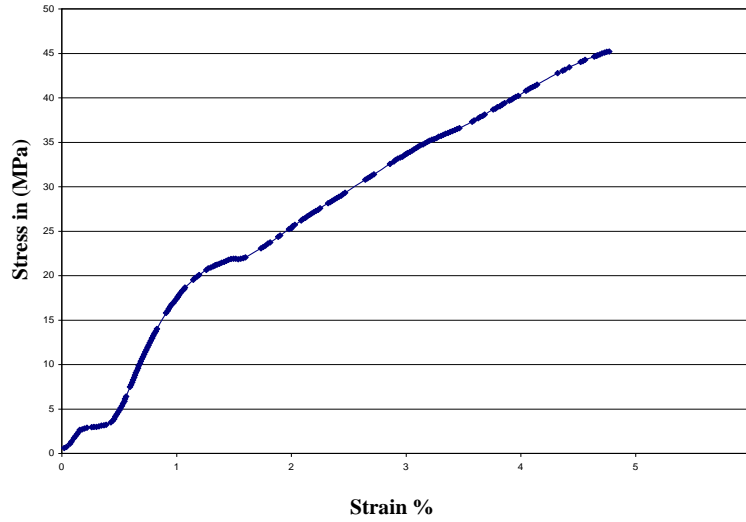


Fig. (10) Stress-Strain curve of Sample (AS43), Atomization pressure = 4 mbar, distance from nozzle =12 cm.

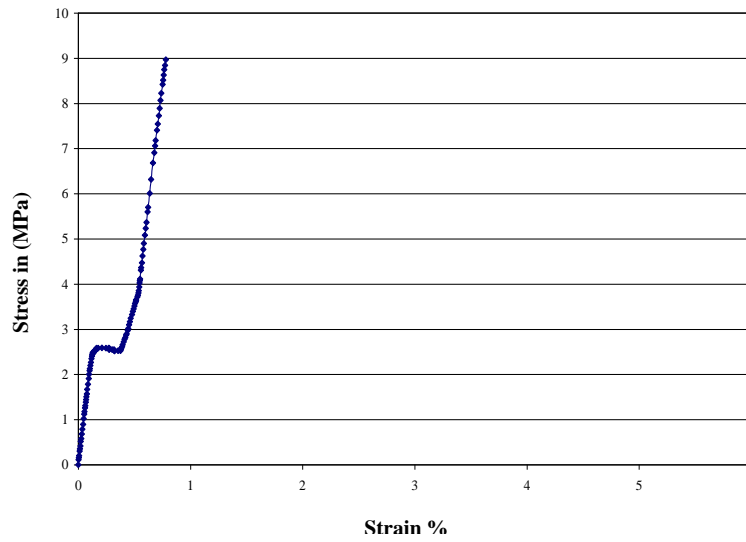


Fig. (11) Stress strain curve of Sample (AS58) Atomization pressure =8 mbar distance from nozzle =12 cm.

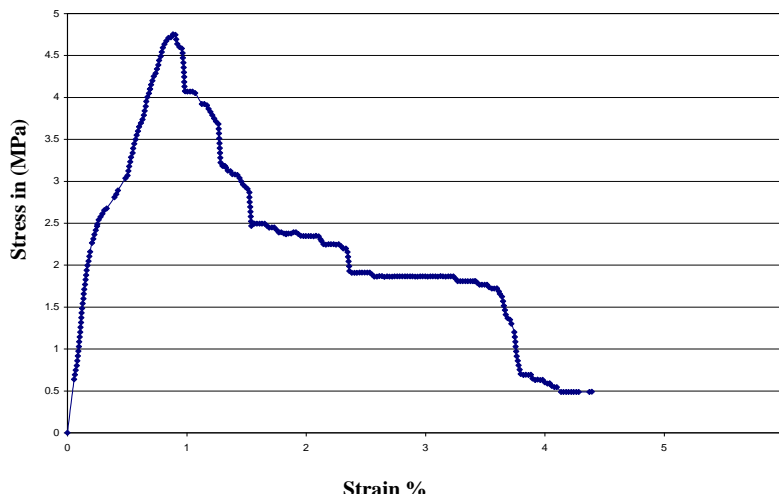


Fig. (12) Stress-strain curve of Sample (AS64), Atomization pressure =3 mbar, distance from nozzle =16 cm.

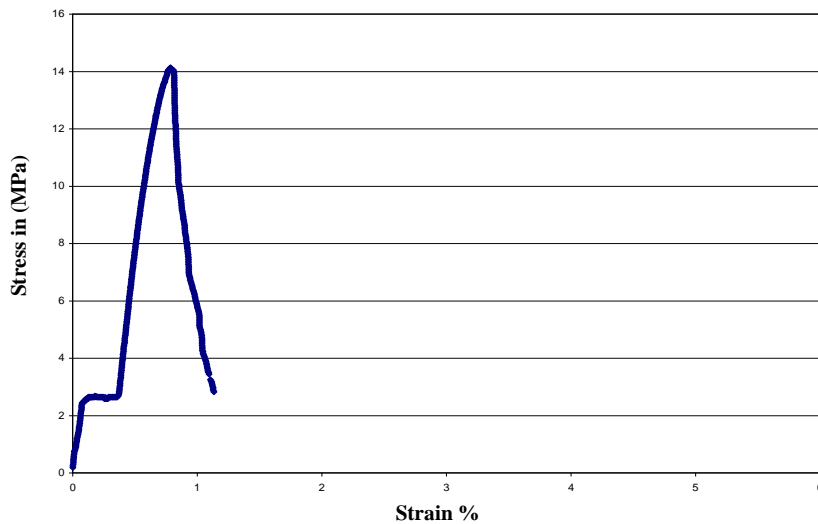


Fig. (13) Stress strain curve of Sample (AS76), atomization pressure =8 mbar distance from nozzle =16 cm.

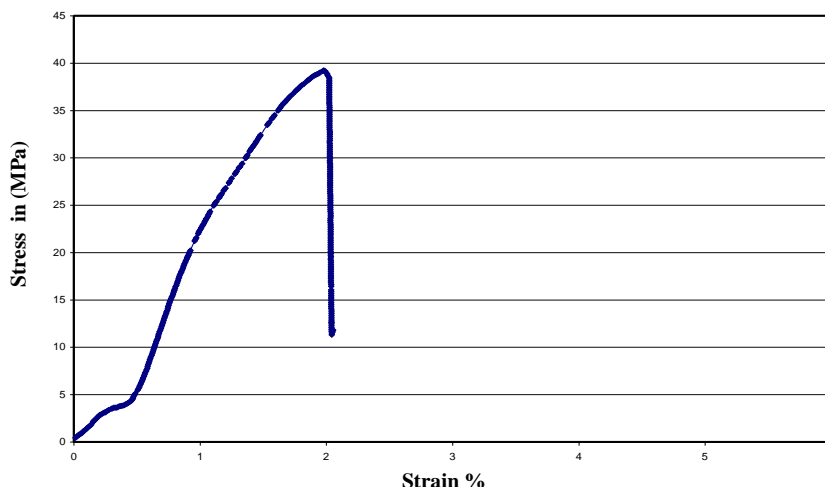


Fig.(14) Stress strain curve of Sample (AS85), Atomization pressure =6 mbar distance from nozzle =18 cm.

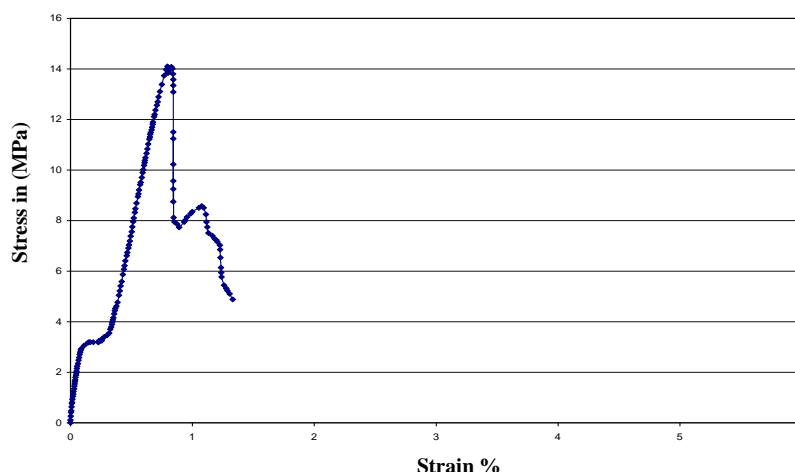


Fig. (15) Stress strain curve of Sample (AS97), atomization pressure =8 mbar distance from nozzle =18 cm.

The Young modulus and tensile strength results of nine samples are shown in table (3).

Table (3) the results of Young modulus and tensile strength of the used samples.

Name of sample	Young Modulus in (MPa)*10 <sup>2</sup>	Tensile strength (MPa)
AS110	49.46	27.99
AS29	28.59	20.22
AS32	22.07	28.9
AS43	29.38	45.28
AS58	19.93	8.96
AS64	14.77	4.747
AS76	39.62	14.17
AS85	38.41	39.27
AS97	24.12	14.08

## Discussion

### 1 .XRD

It's obviously from Fig. (5) and (6) that no oxidation has been occurred in spite of using air in the atomization process. This can be explained by: first, the atomized melt doesn't exposed to the atomization air just for only a little time, about 0.15 s knowing the velocity of melt from [6] about 0.83 m/s. second, the melt cooling is extremely fast in the atomization process. The other note about the Fig.s is the disintegrated melt is only formed from aluminum without copper this can be explained by knowing that the run temperature of the system was 750 °C; which is lower than the copper melting temperature, so the copper doesn't go down with the atomized melt and it stays with other high viscous melts.

### 2. Mechanical properties

#### 2.1 Tensile strength

From Fig.s 7 to 15 of the stress-strain curves of the samples AS110 through AS97 and from the results in Table (3) it's clear that the atomization pressure and the sample distance have an important effect on the mechanical tensile properties. Generally from the curves there are a small deflection from the straight line in the beginning of elastic region, this generally dismissed as being due to the specimen 'settling down' in the

grips, machine backlash being taken up, slippage and so on, its neglected in calculating the Young modulus [7]. It's noticed that with increasing atomization pressure from 4 to 8 in the samples number (AS43, AS32 & AS29) the tensile strength becomes lesser at the same value of nozzle to sample distance. This can be related to porosity forming mechanisms. If the atomization pressure is increased beyond certain value, although this will effectively decrease the droplet size formed during atomization, but the higher quench rate associated with smaller droplet diameters will promote extensive presolidifications prior to impact with the deposition surface. As a result of the high presolidification an interstitial porosity formed in a high rate, which in turn leads to damping in mechanical properties; specially tensile strength. Another reason for tensile strength damping with increasing atomization pressure is the residual stresses that formed due to high-speed impacts of molten particles or semisolid particles which induce a "peening effect" on the underlying sprayed layer. These reasons also give the explanation of the difference in tensile strength between samples (AS85 and AS97). When the atomization pressure is made below 4 mbar as in sample AS64, the disintegrated melt particles will be large, and due to the reduction in volume of the deposited material during solidification the solidification porosity occurred. This lead to the damping in tensile strength [2]. In the case of constant pressure as in samples number (AS76, AS97, AS58 & AS29). For these samples Table (3) reveals that with decreasing the distance between the nozzle and sample plate the tensile strength is increased, excluding sample AS58. This is due to the residual stresses that came from thermal stresses and the quenching stresses. Thermal stresses occurred due to the thermal mismatch between the coating and substrate that takes place during the

postdeposition cooling to room temperature, adding to it the rapid quenching of splats by the substrate. Thermal stresses,  $\sigma_{TC}$ , can be estimated with the aid of the equation:

$$\sigma_{TC} = \Delta\alpha\Delta TE_o \quad (1)$$

where  $\Delta\alpha$  is the the coefficient of thermal expansion (CTE) mismatch between the coating and substrate, and  $\Delta T$  is the temperature difference upon postdeposition cooling. The maximum quenching residual stress is given by:

$$\sigma_{max} = \alpha_o\Delta TE_o \quad (2)$$

Where  $\alpha_o$  and  $E_o$  are the coefficient of thermal expansion (CTE) and elastic modulus of the coating respectively, and  $\Delta T = T_m - T_s$  with  $T_m$  being the melting temperature of the coating and  $T_s$  the substrate temperature. In the case of these samples the cause of the difference in the formed residual stresses came from the difference in  $\Delta T$  among them. For sample AS29  $\Delta T$  is smaller than the others because the substrate plate is closer to the furnace edge so its temperature is higher than the others. And for sample AS76 the substrate temperature is higher than in sample AS97, so  $\Delta T$  is smaller. In sample AS58  $\Delta T$  is smaller than that in samples AS76 and AS97, but the peeing effect resulted from the high impact particle velocities may lead to this damping in the mechanical properties. The peeing effect doesn't affect sample AS29 much because of the high substrate temperature. So the sample which has the minimum  $\Delta T$  will have the minimum residual stress, in the absence of the peeing effect, and accordingly will have the higher tensile strength. Taking samples AS29 and AS110 from Table 3 it can be noted that the sample with no reinforcement (sample AS110) have higher tensile strength in spite of the same preparing conditions. The reason after that is the residual stress in sample AS29 is came from the thermal stress given by equation (1) plus the quenching stress given by equation (2). While in sample AS110 the

residual stress is came only from the quenching stress given by equation (2) [2].

## 2.2 Young Modulus

From Table (3) it can be observed that the best result was to the unreinforced sample AS110; this is due to the weak bond interaction between aluminum and steel carbon fiber [8]. The weak interaction may lead to trap gas molecules in the interface region between steel fiber and Aluminum particles and causes porosity increasing. The Young modulus is proved to be decreased with porosity increasing [9]. Taking samples AS32, AS43 & AS29 as pressure increased from 4 mabr to 5 mabr the Young modulus decreased this may be due to increasing interstitial porosity that formed due to presolidification, as stated before, which leads to Young modulus decreasing. The sudden increase that occurred in sample AS29 (at pressure 8 mbar) is due to increasing the impact velocity of droplets which improve the pore-filling capacity of droplets, and thus substantially reduce the porosity and improve adhesion with the fiber and cohesion between particles [2]. In the case of constant pressure as in samples number (AS76, AS97, AS58 & AS29), as distance increased from (12) to (14) the Young modulus is decreased due to the peeing effect that appears in the distance of 14 cm more than the 12 cm because the substrate temperature is higher in the case of sample to nozzle distance equal to 12 cm, so the peeing effect is lessened. As the sample to nozzle distance increased from 14 cm to 16 cm the Young modulus is increased; this rising is explained by knowing that the droplet velocity is decreased as its path in air increased, so the peeing effect is reduced with distance increasing so the residual stress is decreased and the cohesion increased between particles. The decrease in Young modulus with further increase in distance is due to high cooling

of particles which lead to low adhesion between aluminum and steel fiber and low cohesion between aluminum particles. Taking samples (AS85 & AS97), it can be noted that the results of Young modulus was better with the pressure 6 mbar than in the case of pressure 8 mbar; this may be due to the effect of peeing residual stress in the case of the pressure 8 mbar.

## 6. Conclusions

- The effect of oxidation is mostly disappeared in spite of using air in the atomization process as appeared from XRD spectrum in Figs. (5) and (6).
- Tensile strength is decreased with increasing distance between nozzle and sample for atomization pressure equal to 8 mbar.
- Tensile strength is decreased with increasing atomization pressure for constant nozzle to substrate distance equal to 12 cm.
- Young modulus is decreased then increased with increasing distance between nozzle and sample.

## References

- [1] T. Shalu, E. Abhilash and M.A. Joseph, J. of Mater. Proc. Tech. 209 (2009) 4809–4813.
- [2] J. R. Groza, J.F. Shackelford, E.J. Lavernia and M.T. Powers "Materials Processing Handbook", Taylor & Francis Groub,USA, 2007.
- [3] M. Gupta, M.O. Lai, C.Y.H. Lim S.W. Lee, J. of Mater. Proc. Tech. 176 (2006) 191–199
- [4] W. Zhang, D. Chai, G. Ran, J. Zhou, Mater. Sci. & Eng. A 476 (2008), 157–161.
- [5] D. Mandala, B.K. Duttab, S.C. Panigrahi, Mater. Sci. & Eng. A 492 (2008), 346–352.
- [6] A. S. F. Khalaf, (Ph.D.) Thesis, The School of Applied Sciences, University of Technology, Baghdad, Iraq, (2008).
- [7] J. M. Hodgkinson, Mechanical testing of advanced fiber composites, pg 63, Woodhead Publishing, Cambridge, England, 2000.
- [8] J.K. Kim and Y.W. Mai: Engineered Interfaces in Fiber Reinforced Composites, (Elsevier Science Ltd, Oxford, U.K.) (1998).
- [9] M. Lubrick, R. G. Maev, F. Severin & V. Leshchynsky, J. Mater. Sci. 43, (2008) 4953-4961.